# DYNAMICS IN THOMPSON'S GROUP $F$

JAMES BELK AND FRANCESCO MATUCCI

Abstract. We describe an explicit relationship between strand diagrams and piecewise-linear functions for elements of Thompson's group $F$. Using this correspondence, we investigate the dynamics of elements of $F$, and we show that conjugacy of one-bump functions can be described by a Mather-type invariant.

Thompson's group $F$ is the group of all piecewise-linear homeomorphisms of the unit interval with finitely many breakpoints and satisfying the following conditions:

(1) Every slope is a power of two, and
(2) Every breakpoint has dyadic rational coordinates.

The group $F$ is finitely presented (with two generators and two relations) and torsion-free. It can be thought of as a "lattice" in the full group $\mathrm{PL}_0(I)$ of orientation-preserving piecewise-linear homeomorphisms of $[0,1]$ with finitely many breakpoints, and indeed it shares many properties with this larger group. Elements of $F$ can be represented as different types of diagrams. We will assume some familiarity with the point of view of *tree diagrams*. See [7] or [3] for an introduction to $F$.

In [4], the authors used the *strand diagrams* to give a unified solution to the conjugacy problems in Thompson's groups $F$, $T$, and $V$. A strand diagram is a certain planar directed graph that describes an element of $F$, similar to a braid but with splits and merges instead of twists. In the present work, we derive an explicit correspondence between strand diagrams and piecewise-linear functions. Specifically, we show that strand diagrams can be interpreted as *stack machines* acting on binary expansions. Using this correspondence, we obtain a complete understanding of the dynamics of elements, giving simple proofs of several previously known results. In addition, we describe a completely dynamical solution to the conjugacy problem for one-bump functions in $F$, similar to the dynamical criterion for

The first author gratefully acknowledges partial support from an NSF Postdoctoral Research Fellowship. This work is part of the second author's PhD thesis. The second author gratefully acknowledges the Centre de Recerca Matemàtica (CRM) and its staff for the support received during the completion of this work.

conjugacy in $\mathrm{PL}_0(I)$ derived by Brin and Squier [6]. We mention related work that uses the dynamical point of view: in 2006 Kassabov and Matucci [12] give a solution to the simultaneous conjugacy problem and in 2007 Gill and Short [8] extended Brin and Squier's criterion to work in $F$.

Many of the results in this paper can also be extended to Thompson's groups $T$ and $V$ (some of this results can be found in [14]). See [4] or [14] for information on strand diagrams for these groups.

This paper is organized as follows: in Section 1 we recall the definition of strand diagrams and describe how to view them as machines. In Section 2 we describe annular strand diagrams as conjugacy invariants and how recover dynamical information from them. In Section 3 we recall the definition of Mather invariant for a function and we prove that they are equivalent to annular strand diagrams for a particular class of functions.

## 1. Strand Diagrams

In this section, we describe how to represent elements of $F$ using strand diagrams. Strand diagrams were first discussed in [3], and they were used in [4] to solve the conjugacy problems in Thompson's groups $F$, $V$, and $T$. For $F$, strand diagrams are dual to the "diagrams" of Guba and Sapir ([11], [10]), and the same as the "monoid pictures" introduced by Pride in [15], [16] and [5].

We present here a new interpretation of strand diagrams as stack machines. This provides a direct link between strand diagrams and piecewise-linear functions and a way for a dynamical understanding of conjugacy. This description was inspired by a similar description of $F$ in [9] as an "asynchronous automata group".

### 1.1. Representation of Elements.

*Strand diagrams* are a different way to represent elements of $F$. A strand diagram is similar to a braid, except instead of twists, there are splits and merges:

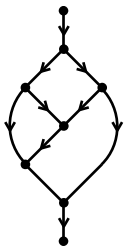

To be precise, a strand diagram is any directed, acyclic graph in the unit square satisfying the following conditions:

(1) There exists a unique univalent source along the top of the square, and a unique univalent sink along the bottom of the square.
(2) Every other vertex lies in the interior of the square, and is either a split or a merge:


As with braids, isotopic strand diagram are considered equal.

Each strand diagram represents a certain piecewise-linear homeomorphism $f\colon I \to I$. The strand diagram is like a computer circuit: whenever a binary number $t \in [0,1]$ is entered into the top, the signal winds its way through the circuit and emerges from the bottom as $f(t)$ (see figure 1).

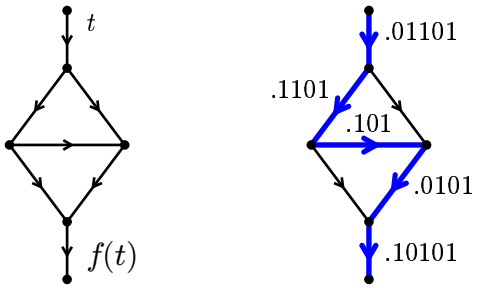


FIGURE 1. A strand diagram as a circuit

During the computation, the binary number changes each time that the signal passes through a vertex. For a split, the signal travels either left or right based on the first digit of the number (figure 2).

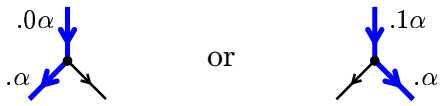


FIGURE 2. Split rule

The first digit is lost after the signal passes through the split. For a merge, the number gains an initial 0 or a 1, depending on whether it enters from the left or from the right (figure 3).

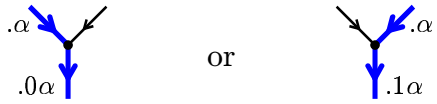


FIGURE 3. Merge rule

This describes the action of a strand diagram on the unit interval. We will show in the next section that every strand diagram acts as an element of $F$.

**Example 1.1.** The following figure shows the three different paths that numbers might take through a certain strand diagram:

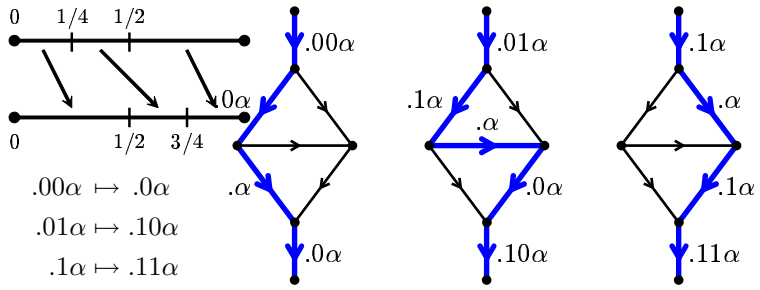


Figure: Three paths through a strand diagram

As you can see, this strand diagram acts as the element of $F$ shown on the left.

**Note 1.2.** The scheme above is really the description of a *stack machine* represented by a strand diagram. A stack machine is similar to a finite-state automaton, except that the input and output are replaced by one or more stacks of symbols. Each state of a stack machine is either a *read state*, *write state*, or a *halt state*. A read state pops a symbol from a stack, and then moves to another state determined by which symbol was read. A write state pushes a symbol onto a stack and then moves to a specified other state. The process ends when the machine moves to a halt state. A strand diagram can be interpreted as a stack machine with one stack. Each edge represents a state of the stack machine. Edges that end with a split are read states, edges that end with a merge are write states, and the edge that ends with the sink is a halt state.

1.2. **Reductions.**

**Definition 1.3.** A *reduction* of a strand diagram is either of the following moves:

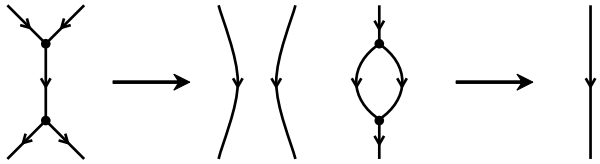


Figure: Reductions for strand diagrams

Neither of these simplifications changes the action of the strand diagram on binary sequences (see figure 4).

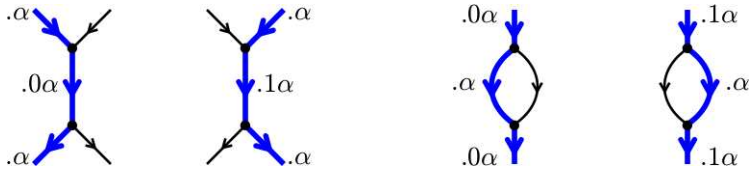


FIGURE 4. Reductions do not change the underlying map

**Proposition 1.4.** *The reduced strand diagrams are in one-to-one correspondence with the elements of $F$. In particular, each reduced strand diagram acts on binary sequences as an element of $F$.* □

The advantage of strand diagrams over tree diagrams is that multiplication is the same as concatenation:

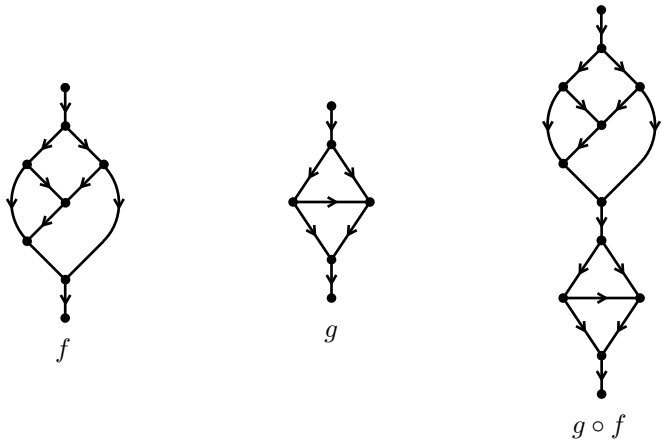

This algorithm is considerably simpler than the standard multiplication algorithm for tree diagrams (see [7]). In [4], the authors used this property of strand diagrams to provide solutions to the conjugacy problems in $F$, $V$, and $T$. (For $F$, this was based on an earlier solution by Guba and Sapir using similar pictures.)

1.3. **$(m,n)$-Strand Diagrams .** We look at the groupoid of $(m,n)$-Strand Diagrams from the dynamical point of view (see figure 5). Recall that

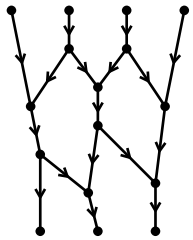

FIGURE 5. An element of Thompson's groupoid

a strand diagram with $m$ sources and $n$ sinks is called an $(m,n)$-*strand diagram*. Such a strand diagram can receive input along any of its sources; the signal then travels through the diagram according to the rules in section 1.1, eventually emerging from one of the sinks.

We can interpret an $(m,n)$-strand diagram as a piecewise-linear homeomorphism $[0,m] \to [0,n]$. Specifically, a number of the form $k + 0.\alpha$ corresponds to an input of $.\alpha$ entered into the $k$th source, or an output of $.\alpha$ emerging from the $k$th sink. The set of piecewise-linear functions determined in this way is precisely the set of dyadic rearrangements from $[0,m]$ to $[0,n]$, i.e. the orientation-preserving homeomorphisms $[0,m] \to [0,n]$ whose slopes are powers of two, and whose breakpoints have dyadic rational coordinates.

The set of homeomorphisms described above is closed under compositions and inverses, and therefore forms a *groupoid* with objects $\{[0,1], [0,2], [0,3], \ldots\}$. Indeed two homeomorphisms $f\colon [0,m] \to [0,m]$ and $g\colon [0,n] \to [0,n]$ from Thompson's groupoid are conjugate if and only if they have the same reduced annular strand diagram (by the results in Chapter 2 of [14]).

## 2. Dynamics of Annular Strand Diagrams

2.1. **Annular Strand Diagrams.** In this section, we provide a short summary of the some of the results from [4]. Given a strand diagram in the

unit square, we can identify the top can bottom to obtain an *annular strand diagram*:

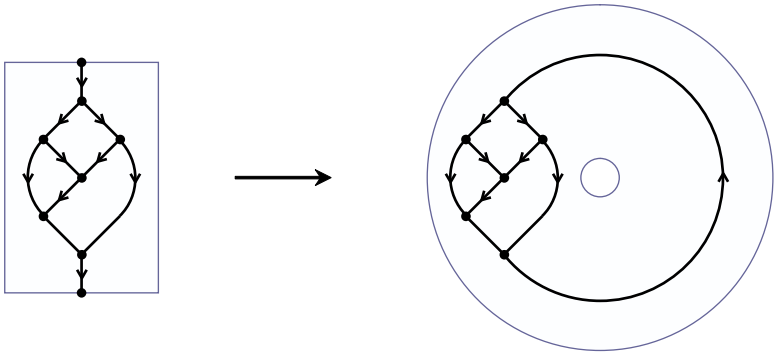

Every vertex of an annular strand diagram is either a split or a merge, and every directed loop has positive index around the central hole. When considering annular strand diagrams, it is important to allow for the possibility of *free loops*—directed loops with no beginning or end vertex.

Annular strand diagrams can be reduced using the moves given in section 1.3, along with an additional move allowing for the combination of concentric free loops:

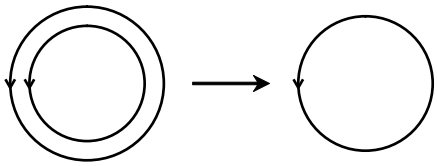

Every annular strand diagram is equivalent to a unique reduced annular strand diagram.

**Theorem 2.1.** *Two elements of $F$ are conjugate if and only if they have the same reduced annular strand diagram.* □

Indeed, two homeomorphisms $f\colon [0,m] \to [0,m]$ and $g\colon [0,n] \to [0,n]$ from Thompson's groupoid are conjugate if and only if they have the same reduced annular strand diagram.

Here is a typical reduced annular strand diagram:

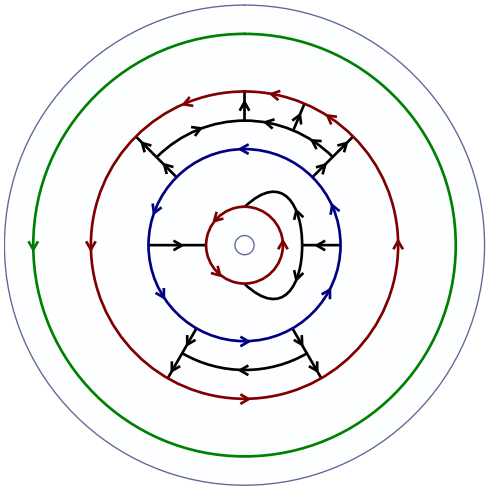

The main features are the large directed cycles winding counterclockwise around the central hole. These cycles are all disjoint, and can be classified into *merge loops* (shown in red), *split loops* (shown in blue), and *free loops* (shown in green). This diagram above has two connected *components*, and a general reduced annular strand diagram may have several concentric components. Within each component, the cycles must alternate between split loops and merge loops.

2.2. **Fixed points and "chaos".** In this section we survey some known results on dynamics in $F$. Figure 6 is the graph for an element of $F$ The main dynamical features of this element are the four fixed points at 0, $\frac{1}{3}$, $\frac{3}{4}$, and 1. Every element of $F$ fixes 0 and 1, but not every element has *interior fixed points* like $\frac{1}{3}$ and $\frac{3}{4}$. We are going to observe the properties of the fixed points of this element by studying the *local replacement rule*: we look at a one-sided neighborhood $U_p$ of a fixed point $p$ that is small enough so that the map $x \to f(x)$ is linear for any $x \in U_p$ and hence, if $x$ is written in binary expansion, then $f(x)$ is obtained by adding some digits in front of $x$ or subtracting some of the first digits of $x$, with the tail of the binary expansion of $x$ and $f(x)$ remaining the same.

(1) The fixed point at 0 is attracting, since the slope is $\frac{1}{2}$. The local replacement rule is $.\alpha \mapsto .0\alpha$, which causes points near zero to converge to zero:

$$.\alpha \mapsto .0\alpha \mapsto .00\alpha \mapsto .000\alpha \mapsto \cdots$$

(2) Fixed points do not have to be dyadic. In fact, the fixed point at $\frac{1}{3}$ is not a dyadic fraction. In binary, the local replacement rule is

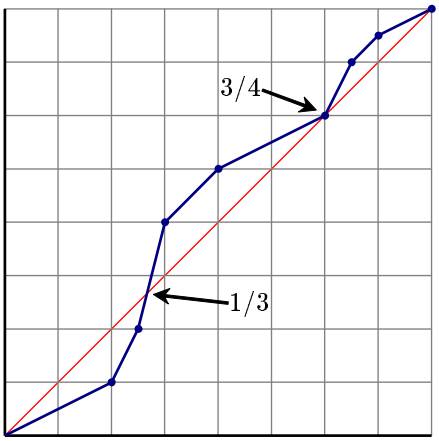


FIGURE 6. An example of an element of $F$

$.10\alpha \mapsto .\alpha$, with a fixed point at $.101010\ldots = \frac{1}{3}$. The slope here is 4, so the fixed point is repelling:

$$.101010\alpha \mapsto .1010\alpha \mapsto .10\alpha \mapsto .\alpha \mapsto \cdots$$

(3) The fixed point at $\frac{3}{4}$ is dyadic, and has two local replacement rules: $.10\alpha \mapsto .101\alpha$ on the left, and $.1100\alpha \mapsto .110\alpha$ on the right. This makes $\frac{3}{4} = .101111\ldots = .110000\ldots$ attracting from the left:

$$.10\alpha \mapsto .101\alpha \mapsto .1011\alpha \mapsto .10111\alpha \mapsto \cdots$$

and repelling from the right:

$$.110000\alpha \mapsto .11000\alpha \mapsto .1100\alpha \mapsto .110\alpha \mapsto \cdots.$$

Only an interior dyadic fixed point can have different behavior from the left and from the right, because only a dyadic rational can be a breakpoint for an element of $F$.

If we think of $F$ as acting on the Cantor set, then $\frac{3}{4}$ corresponds to *two* fixed points of $f$: one at .101111 and the other at .110000. Each of these fixed points has a well-defined slope.

(4) The fixed point at 1 is attracting, with local replacement rule $.\alpha \mapsto .1\alpha$.

If we think of $F$ as acting on the Cantor set, then each fixed point of an element of $F$ has a well-defined slope, because dyadic rational fixed points are counted twice (as they can have different slopes on the right and on the left). The possible values of this slope depend on the tail of the fixed point:

**Proposition 2.2.** *Suppose that $f \in F$ has a fixed point at $t$, and let $n$ be the eventual period of the binary expansion for $t$. Then the slope of $f$ on each side of $t$ is an integer power of $2^n$. If $t$ is non-dyadic, the slopes at the two sides must be equal.*

*Proof.* By hypothesis, $t = .\mu\overline{\rho}$, where $\rho$ is a binary sequence of length $n$. If $\mu$ is as short as possible, then any element of $F$ with a fixed point at $t$ must have the local replacement rule

$$.\mu\rho^k\alpha \longmapsto .\mu\alpha \quad \text{or} \quad .\mu\alpha \longmapsto .\mu\rho^k\alpha$$

near $t$, for some $k \geq 0$. The first case gives a slope of $(2^n)^k$, and the second a slope of $(2^n)^{-k}$. □

For example, any element of $F$ that fixes $1/3$ must have slope $4^n$ at the fixed point. Because a dyadic rational has eventual period 1, the left and right slopes at a dyadic fixed point can be any powers of 2.

Most of the properties of the fixed points are preserved under conjugation:

**Proposition 2.3.** *Let $f, g \in F$, and suppose that $f$ has fixed points at*

$$0 = t_0 < t_1 < \cdots < t_n = 1.$$

*Then $gfg^{-1}$ has fixed points at*

$$0 = g(t_0) < g(t_1) < \cdots < g(t_n) = 1.$$

*Moreover, the slopes of $gfg^{-1}$ on the left and on the right of $g(t_i)$ are the same as the slopes of $f$ on the left and on the right of $t_i$.*

*Proof.* This is very elementary. The statement about slopes follows from the chain rule. □

Thus it makes sense to talk about the "number of fixed points" for a conjugacy class of $F$, as well as the "slope at the 5th fixed point". The following proposition lets us talk about the "tail of a fixed point":

**Proposition 2.4.** *Let $t, u \in (0, 1)$. Then $t$ and $u$ are in the same orbit of $F$ if and only if $t$ and $u$ have binary expansions with the same tail—that is, if and only if*

$$t = .\mu\omega \qquad \text{and} \qquad u = .\nu\omega$$

*for some finite binary sequences $\mu, \nu$ and some infinite binary sequence $\omega$.*[1]

*Proof.* For the forward direction, observe that any replacement rule preserves the tail of a binary sequence. For the backwards direction, it is easy to draw a "pipeline" that implements the rule $.\mu\alpha \mapsto .\nu\alpha$ (see figure 7).

[1]This result cannot be extended to generalized Thompson's groups. In fact, while Thompson's group $F$ is transitive on all dyadic rational points, this is not true anymore for generalized Thompson's groups and $n$-adic rational points: see Chapter 4 in [14], Remark 4.4.9.

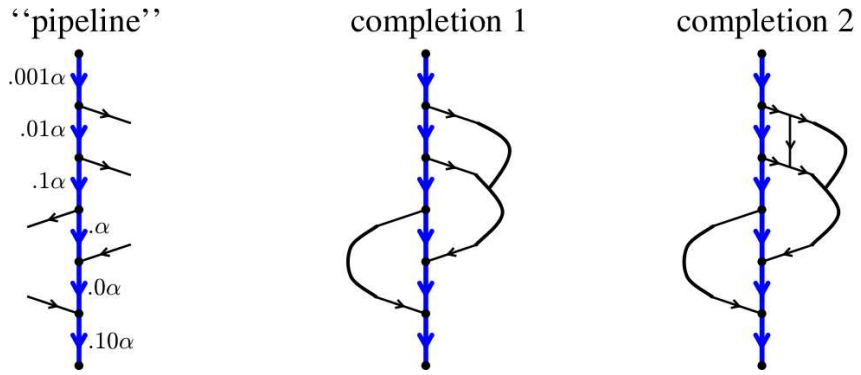


FIGURE 7. Completing an element out of a "pipeline"

Up to taking the common tail to start from a further digit, we can assume $\mu$ and $\nu$ each have both 0's and 1's (i.e. both left and right connections), otherwise $.\mu\alpha$ or $.\nu\alpha$ is 0 or 1. This drawing can easily be extended to a complete strand diagram by adding strands on the left and on the right so that all the outgoing strands can be suitably arranged to get into the ingoing ones. Figure 7 shows two possible ways to complete the pipeline, leading to two distinct elements of $F$. □

For example, the image of $\frac{3}{4}$ under an element $g \in F$ can be any dyadic fraction, and the image of $\frac{1}{3}$ can be any rational number whose binary expansion ends in $010101\ldots$ (i.e. any number whose difference from $\frac{1}{3}$ is dyadic). The previous result can be obtained using the language of piecewise-linear homeomorphisms (see Chapter 4 in [14]).

The following proposition shows that there are no further constraints on the positions of the fixed points within a conjugacy class:

**Proposition 2.5.** *Let $0 = t_0 < \cdots < t_n = 1$ and $0 = u_0 < \cdots < u_n = 1$, and suppose that each $t_i$ is in the same $F$-orbit as the corresponding $u_i$. Then there exists an element of $F$ that maps $(t_0, \ldots, t_n)$ to $(u_0, \ldots, u_n)$.*

*Sketch of the Proof.* A strand diagram for the required element can be constructed using a method similar to the proof of the previous proposition. □

2.3. **Cut Paths and Thompson's Groupoid.** Thompson's groupoid is fundamental to the study of conjugacy in $F$. For example, figure 8 shows three strand diagrams that represent conjugate elements of $F$. Each of these elements begins by partitioning $[0, 1]$ into four subintervals, and ends by recombining these four subintervals into $[0, 1]$. They differ only in the choice of the partition. These elements are all conjugate to the element of

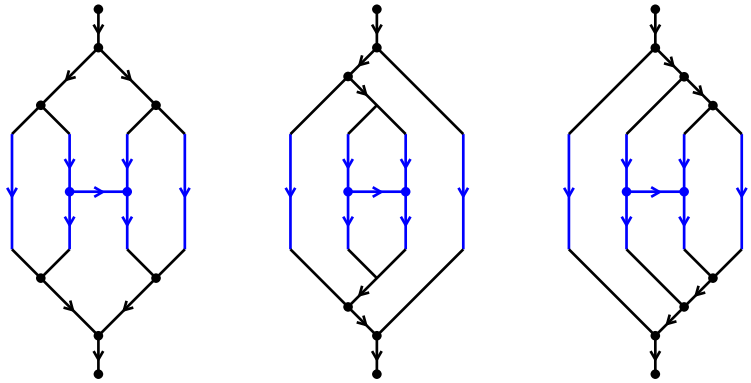

FIGURE 8. Three conjugate elements

Thompson's groupoid shown in figure 9. As you can see, this homeomor-

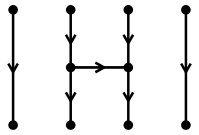

FIGURE 9. A minimal representative

phism $[0,4] \to [0,4]$ is simpler than any of the elements of $F$ above. Indeed, this element is a *minimal* representative for its conjugacy class, in the sense that it is reduced (it has the fewest possible splits and merges). The reason is that any element of this conjugacy class must have at least as many splits and merges as the reduced annular strand diagram of figure 10.

In general, a *cut path* in an annular strand diagram is a path between the outside and the inside of the annulus, with the property that cutting along the cut path yields a strand diagram in the square. (See [4] or [14] for a precise definition.) The minimal representatives of a conjugacy class are precisely those obtained by cutting the reduced annular strand diagram along some cut path.

2.4. **Directed Loops and Fixed Points.** It is possible for an element of $F$ to have infinitely many fixed points. For example, the identity element fixes the entire interval $[0,1]$, and any element of $F$ can have a linear segment that coincides with the identity on some interval $[d,e]$ ($d$ and $e$ dyadic). If $f \in F$, a *fixed interval* of $f$ is either

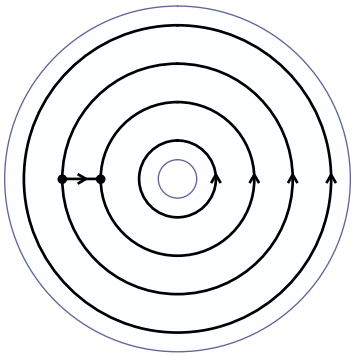

FIGURE 10. The corresponding reduced annular strand diagram

(1) An isolated fixed point $\{t\}$ of $f$, or
(2) A maximal open interval of fixed points,
(3) An endpoint of a maximal open interval of fixed points.

**Convention 2.6.** Each isolated interior dyadic fixed point of $f$ corresponds to two fixed intervals.

**Theorem 2.7.** *Let $f \in F$, and let $S$ be the reduced annular strand diagram for $f$. Then the directed loops $L_0, \ldots, L_n$ of $S$ (ordered from outside to inside) are in one-to-one correspondence with the fixed intervals $I_0 < \cdots < I_n$ of $f$. This correspondence has the following properties:*

(1) *Every free loop corresponds to a maximal interval of fixed points.*
(2) *Every split loop corresponds to an isolated repeller. In particular, a split loop with $n$ splits corresponds to a fixed point with slope $2^n$.*
(3) *Every merge loop corresponds to an isolated attractor. In particular, a merge loop with $n$ merges corresponds to a fixed point with slope $2^{-n}$.*

*In the latter two cases, the pattern of outward and inward connections around the loop determines the tail of the binary expansion of the fixed point. Specifically, each outward connection corresponds to a* 1*, and each inward connection corresponds to a* 0*.*

*Proof.* We have already shown that all of the information outlined in the statement of the theorem is conjugacy invariant. Therefore, we may replace $f$ by any element whose reduced annular strand diagram is $S$. Specifically, we may assume that $f$ is the dyadic rearrangement $[0, k] \to [0, k]$ obtained by cutting $S$ along a cutting path $c$.

$S$ contains a merge loop: some of the vertices on this loop are coming from the inner part of the loop, while some are coming from the outer part of

the loop. We work out an example in detail. The general procedure follows closely from it, as it will become apparent that the general case does not depend on the number of vertices on the loops. Suppose that $S$ contains the merge loop in figure 11. The cutting path $c$ cuts through this loop

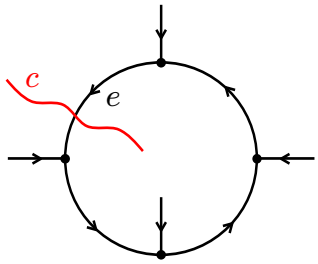


FIGURE 11. An example of a merge loop

exactly once, along some edge $e$. If we place a binary number $.\beta$ along $e$, the number will trace a directed path through the annular strand diagram, changing in value every time it passes through a vertex. Assuming that $c$ crosses $i$ edges before crossing $e$, this corresponds to feeding $i + .\beta$ into the strand diagram for $f$.

In the case we are considering, the number will simply travel around the merge loop (see figure 12). By the time it returns to $e$, its value will be the

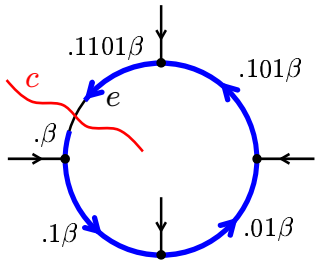


FIGURE 12. Traveling through the merge loop

fractional part of $f\big(i + .\beta\big)$. If we continue following the number along the merge loop, the values it has when it passes through $e$ will be the fractional parts of the iterates $f^n(i+.\beta)$. In the case that we are considering, it follows that:

$$f(i + .\beta) = i + .1101\beta \quad f^2(i + .\beta) = i + .1101\,1101\beta \quad \text{etc.}$$

In particular, the number $\alpha = i + .\overline{1101}$ is a fixed point of $f$.

Note that the sequence 1101 is determined by the counterclockwise pattern of inward and outward edges, exactly as stated in the theorem. In addition, we have shown that $f$ is linear on $[i, i+1]$, with formula:

$$f(i + .\beta) \;=\; i + .1101\,\beta.$$

This linear function has slope $2^{-4}$. This implies that $\alpha$ is an attracting fixed point—indeed, for any $i + .\beta \in [i, i+1]$, the first $4n$ digits of $f^n(i + .\beta)$ are the same as the first $4n$ digits of $\alpha$.

A split loop works in roughly the same way, except that a split loop is repelling (see figure 13). Note that every fixed point of $f$ arises from either

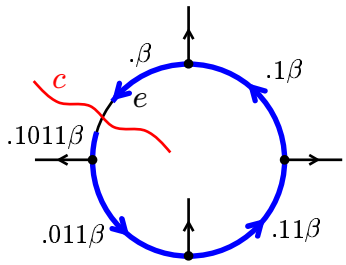


FIGURE 13. An example of a split loop

a split loop or merge loop. In particular, suppose that $i + .\beta$ is a fixed point of $f$, and let $e$ be the $(i+1)$'st edge crossed by $c$. If we place the binary number $.\beta$ along $e$, then the resulting path of motion must wind once around the central hole and then return to $e$ with value $.\beta$. It follows that $.\beta$ must have traveled around a directed loop, and $i + .\beta$ is the unique fixed point determined by the loop. □

Note that the outermost loop of an annular strand diagram for $f \in F$ corresponds to the fixed point $0 = .0000\cdots$, while the innermost loop corresponds to the fixed point $1 = .1111\cdots$. Within each connected component of $S$, the outermost and innermost loops correspond to dyadic fixed points, while the interior loops correspond to non-dyadic fixed points.

**Corollary 2.8.** *Let $S$ be the reduced annular strand diagram for an element $f \in F$. Then every component of $S$ corresponds to exactly one of the following:*

(1) *A maximal open interval of fixed points of $f$ (for a free loop), or*
(2) *A maximal interval with no dyadic fixed points of $f$ in its interior.*

If $f \in F$, a *cut point* of $f$ is either an isolated dyadic fixed point of $f$, or an endpoint of a maximal interval of fixed points. If $0 = \alpha_0 < \alpha_1 < \cdots < \alpha_n = 1$ are the cut points of $f$, then the restrictions $f_i \colon [\alpha_{i-1}, \alpha_i] \to [\alpha_{i-1}, \alpha_i]$ are called the *components* of $f$ (see figure 14). Each component of

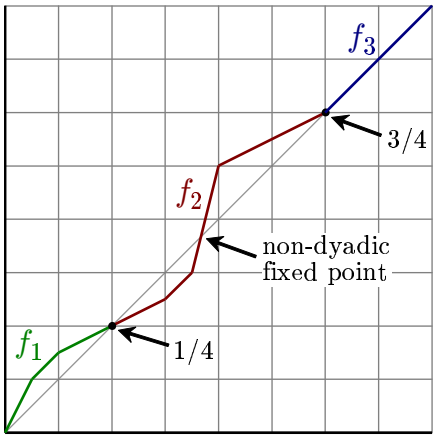


FIGURE 14. Components of a function

$f$ corresponds to one connected component of the reduced annular strand diagram(figure 15).

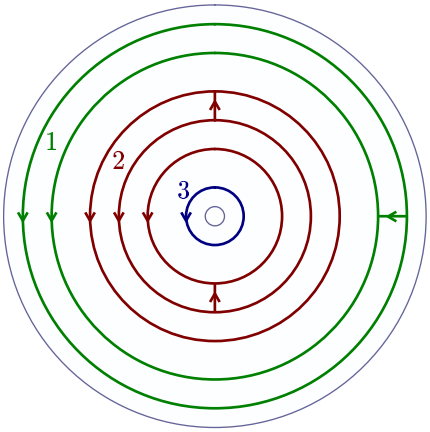


FIGURE 15. Annular strand diagram for a component

If $\alpha < \beta$ are any dyadic rationals, it is well known (see [7] or [14]) that there exists a Thompson-like homeomorphism $\varphi\colon [\alpha, \beta] \to [0, 1]$ (i.e. a piecewise-linear homeomorphism whose slopes are powers of 2, and whose breakpoints have dyadic rational coordinates). It follows that any Thompson-like homeomorphism of $[\alpha, \beta]$ can be conjugated by $\varphi$ to give an element of $F$.

**Proposition 2.9.** *Let $f \in F$ have components $f_i\colon [\alpha_{i-1}, \alpha_i] \to [\alpha_{i-1}, \alpha_i]$, and let $S$ be the reduced annular strand diagram for $f$. Then for each $i$, the component of $S$ corresponding to $f_i$ is the reduced annular strand diagram for any element of $F$ conjugate to $f_i$.*

*Proof.* Suppose $f$ has $n+1$ cut points $0 = \alpha_0 < \alpha_1 < \cdots < \alpha_n = 1$. Then we can conjugate $f$ to an element of Thompson's groupoid whose cut points are at $0, 1, 2, \ldots, n$. The resulting $(n, n)$-strand diagram has $n$ connected components which, when reduced, yield the $n$ components of $S$. □

**Corollary 2.10.** *Let $f, g \in F$ have components $f_1, \ldots, f_n$ and $g_1, \ldots, g_n$. Then $f$ is conjugate to $g$ in $F$ if and only if each $f_i$ is conjugate to $g_i$ through some Thompson-like homeomorphism.*

## 3. Mather Invariants

Conjugacy in $F$ was first investigated by Brin and Squier [6], who successfully found a criterion for conjugacy in the full group of piecewise-linear homeomorphisms of the interval. This solution was based on some ideas of Mather [13] for determining whether two given diffeomorphisms of the unit interval are conjugate.

In this section we show that the solution shown in [4] can be described in a way similar to the solutions given by Mather for $\mathrm{Diff}_+(I)$ and by Brin and Squier for $\mathrm{PL}_+(I)$. Specifically, we define a Mather-type invariant for elements of $F$, and show that two one-bump functions in $F$ are conjugate if and only if they have the same Mather invariant.

A somewhat different dynamical description of conjugacy in $F$ has been obtained independently by Gill and Short [8].

### 3.1. Background on Mather Invariants.

Consider the group $\mathrm{Diff}_+(I)$ of all orientation-preserving diffeomorphisms of $[0, 1]$.

**Definition 3.1.** A *one-bump function* is an element $f \in \mathrm{Homeo}_+(I)$ such that $f(x) > x$ for all $x \in (0, 1)$.

Figure 16 shows an example of a one-bump function. By the chain rule, two one-bump functions $f, g \in \mathrm{Diff}_+(I)$ can only be conjugate if $f'(0) = g'(0)$ and $f'(1) = g'(1)$, but this condition is not sufficient. In 1973, Mather

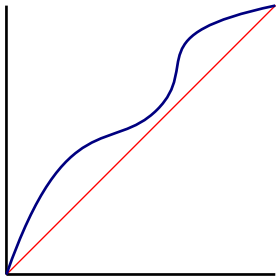

FIGURE 16. A one-bump function

constructed a more subtle conjugacy invariant of one-bump functions $f$ such that $f'(0) > 1$ and $f'(1) < 1$, and proved that two such one-bump functions in $\mathrm{Diff}_+(I)$ are conjugate if and only if they have the same slopes at 0 and 1 and the same Mather invariant. In 1995, Yocozz extended this to a complete criterion for conjugacy in $\mathrm{Diff}_+(I)$ [17]. Similar invariants are used for conjugacy of diffeomorphisms in [2], [18], and [1], the last of which introduces the term "Mather invariant".

In 2001 [6], Brin and Squier [2] extended Mather's analysis to the group $\mathrm{PL}_+(I)$ of all orientation-preserving piecewise-linear homeomorphisms of $[0, 1]$. Specifically, they defined a Mather invariant for one-bump functions in $\mathrm{PL}_+(I)$, and showed that two one-bump functions are conjugate if and only if they have the same slopes at 0 and 1 and the same Mather invariant. Using this result, they went on to describe a complete criterion for conjugacy in $\mathrm{PL}_+(I)$.

The Mather invariant is simpler to describe in the piecewise-linear case. The following description is based on the geometric viewpoint introduced in [18] and [1], so the language differs considerably from that used in [6] or [13].

Consider a one-bump function $f \in \mathrm{PL}_+(I)$, with slope $m_0$ at 0 and slope $m_1$ at 1. In a neighborhood of zero, $f$ acts as multiplication by $m_0$; in particular, for any sufficiently small $t > 0$, the interval $[t, m_0 t]$ is a fundamental domain for the action of $f$ (see figure 17). If we make the identification $t \sim m_0 t$ in the interval $(0, \epsilon)$, we obtain a circle $C_0$, with partial covering map $p_0 \colon (0, \epsilon) \to C_0$. Note that the restriction of $f$ is a

[2]Brin and Squier originally developed this theory in 1987, but it was published in 2001.


FIGURE 17. Action of $f$ in a neighborhood of 0

deck transformation of this cover:

$$\begin{array}{ccc} (0,\epsilon) & \xrightarrow{\quad f \quad} & (0,\epsilon) \\ & {\scriptstyle p_0}\searrow \quad \swarrow{\scriptstyle p_0} & \\ & C_0 & \end{array}$$

Similarly, if we identify $(1-t) \sim (1-m_1 t)$ on the interval $(1-\delta, 1)$, we obtain a circle $C_1$, with partial covering map $p_1 \colon (1-\delta, 1) \to C_1$.

If $N$ is sufficiently large, then $f^N$ will take some lift of $C_0$ to $(0,\epsilon)$ and map it to the interval $(1-\delta, 1)$. This induces a map $f^\infty \colon C_0 \to C_1$, making the following diagram commute:

$$\begin{array}{ccc} (0,\epsilon) & \xrightarrow{\quad f^N \quad} & (1-\delta, 1) \\ \Big\downarrow{\scriptstyle p_0} & & \Big\downarrow{\scriptstyle p_1} \\ C_0 & \xrightarrow{\quad f^\infty \quad} & C_1 \end{array}$$

**Definition 3.2.** The map $f^\infty$ defined above is the Mather invariant for $f$.

We note that $f^\infty$ does not depend on the specific value of $N$ chosen. Any map $f^m$, for $m \geq N$, induces the same map $f^\infty$. This is because $f$ acts as the identity on $C_1$ by construction and $f^m$ can be written as $f^{m-N}(f^N(t))$, with $f^N(t) \in (1-\delta, 1)$. If $k > 0$, then the map $t \mapsto kt$ on $(0,\epsilon)$ induces a "rotation" $\mathrm{rot}_k$ of $C_0$. In particular, if we use the coordinate $\theta = \log t$ on $C_0$, then

$$\mathrm{rot}_k(\theta) \;=\; \theta + \log k$$

so $\mathrm{rot}_k$ is an actual rotation.

**Theorem 3.3** (Brin and Squier)**.** *Let $f, g \in \mathrm{PL}_+(I)$ be one-bump functions with $f'(0) = g'(0) = m_0$ and $f'(1) = g'(1) = m_1$, and let $f^\infty, g^\infty \colon C_0 \to C_1$ be the corresponding Mather invariants. Then $f$ and $g$ are conjugate if and*

*only if $f^\infty$ and $g^\infty$ differ by rotations of the domain and range circles:*

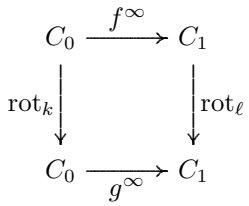


*Proof.* We will show here that conjugate elements have similar Mather invariants. See [6] for the converse.

Suppose that $f = h^{-1}gh$ for some $h \in \mathrm{PL}_+(I)$. Then the following diagram commutes, where $k = h'(0)$ and $\ell = h'(1)$:

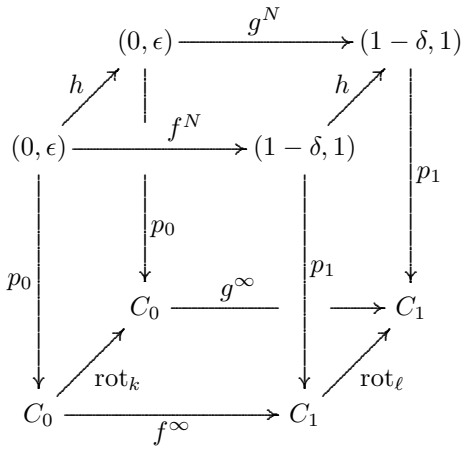


□

For diffeomorphisms, one-bump functions are not linear in neighborhoods of 0 and 1, but it is still possible to define the Mather invariant by taking a limit as $t \to 0$ and $t \to 1$. (Essentially, a one-bump function in $\mathrm{Diff}_+(I)$ acts linearly on infinitesimal neighborhoods of 0 and 1.) In this case, the Mather invariant is a $C^\infty$ function $C_0 \to C_1$.

**Theorem 3.4** (Mather, Young)**.** *Two one-bump functions $f, g \in \mathrm{Diff}_+(It)$ with the same slopes at 0 and 1 are conjugate if and only if $f^\infty$ and $g^\infty$ differ by rotations of the domain and range.*

3.2. **Mather Invariants for $F$ .** In this section, we show that the reduced annular strand diagram for a one-bump function in $F$ can be interpreted as a Mather invariant. Therefore, two one-bump functions in $F$ are conjugate in $F$ if and only if they have the same Mather invariant. We also briefly describe the dynamical meaning of reduced annular strand diagrams for more

complicated elements, thereby giving a completely dynamical description for conjugacy in $F$.

**Definition 3.5.** The *piecewise-linear logarithm* $\mathrm{PLog}\colon (0,\infty) \to (-\infty,\infty)$ is the piecewise-linear function that maps the interval $\left[2^k, 2^{k+1}\right]$ linearly onto $[k, k+1]$ for every $k \in \mathbb{Z}$ (see figure 18).

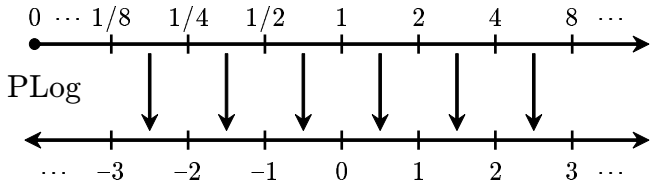


FIGURE 18. The PLog map

Suppose that $f \in F$ is a one-bump function with slope $2^m$ at 0 and slope $2^{-n}$ at 1, and let $f^\infty\colon C_0 \to C_1$ be the corresponding Mather invariant. In a neighborhood of 0, the function $f$ acts as multiplication by $2^m$. In particular, $\mathrm{PLog}\, f(t) = m + \mathrm{PLog}\, t$ for all $t \in (0,\epsilon)$, so we can identify $C_0$ with the circle $\mathbb{R}/m\mathbb{Z}$. Figure 19 shows the case $m = 3$: In a similar way, we

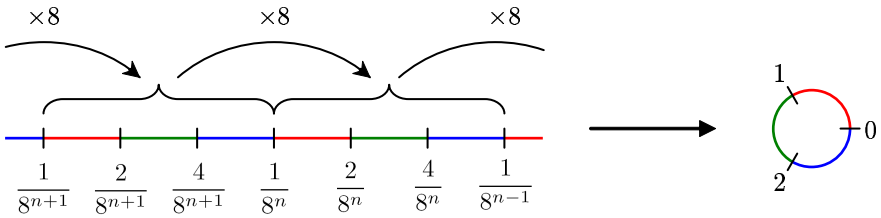


FIGURE 19. Construction of the circle $C_0$

can use the function $t \mapsto -\mathrm{PLog}(1-t)$ to identify $C_1$ with the circle $\mathbb{R}/n\mathbb{Z}$. This lets us regard the Mather invariant for $f$ as a function $f^\infty\colon \mathbb{R}/m\mathbb{Z} \to \mathbb{R}/n\mathbb{Z}$. Because $f^N$ and PLog are piecewise-linear, the Mather invariant $f^\infty$ is a piecewise-linear function. Moreover, $f^\infty$ is Thompson-like: all the slopes are powers of 2, and the breakpoints are dyadic rational numbers of $\mathbb{R}/m\mathbb{Z} = [0,m]/\{0,m\}$.

Now, if $k \in \mathbb{Z}$, then the map $t \mapsto 2^k t$ on $(0,\epsilon)$ induces a "rotation" of $C_0$. Using our new scheme, this is precisely an integer rotation of $\mathbb{R}/m\mathbb{Z}$:

$$\mathrm{rot}_k(\theta) = \theta + k \mod m$$

We are now ready to state the main theorem:

**Theorem 3.6.** *Let $f, g \in F$ be one-bump functions with $f'(0) = g'(0) = 2^m$ and $f'(1) = g'(1) = 2^{-n}$, and let $f^\infty, g^\infty \colon \mathbb{R}/m\mathbb{Z} \to \mathbb{R}/n\mathbb{Z}$ be the corresponding Mather invariants. Then $f$ and $g$ are conjugate if and only if $f^\infty$ and $g^\infty$ differ by integer rotations of the domain and range circles:*

$$\begin{array}{ccc} \mathbb{R}/m\mathbb{Z} & \xrightarrow{f^\infty} & \mathbb{R}/n\mathbb{Z} \\ {\scriptstyle \mathrm{rot}_k}\downarrow & & \downarrow{\scriptstyle \mathrm{rot}_\ell} \\ \mathbb{R}/m\mathbb{Z} & \xrightarrow{g^\infty} & \mathbb{R}/n\mathbb{Z} \end{array}$$

The forward direction follows from the same argument given for proposition 3.3. The converse is more difficult: we must show that any two one-bump functions whose Mather invariants differ by integer rotation are conjugate in $F$. To prove this, we describe an explicit correspondence between Mather invariants and reduced annular strand diagrams.

If $f \in F$ is a one-bump function, then the only fixed points of $f$ are at 0 and 1. Therefore, the reduced annular strand diagram for $f$ has only two directed cycles (see figure 20). Since $f'(0) > 1$, the outer cycle (corresponding to 0) must be a split loop, and the inner cycle (corresponding to 1) must be a merge loop. If we remove these two cycles, we get an $(m, n)$-strand diagram drawn on a cylinder (see figure 21). In [4], this is referred to as a *cylindrical strand diagram*. Such a diagram can be used to describe a Thompson-like map between two circles.

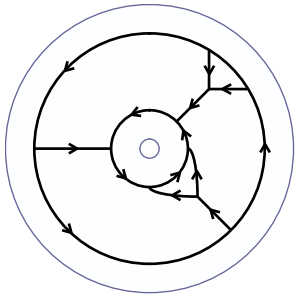

FIGURE 20. Annular strand diagram for a one-bump function

**Proposition 3.7.** *There is a one-to-one correspondence between*

1. *Reduced cylindrical $(m, n)$-strand diagrams, and*
2. *Thompson-like functions $\mathbb{R}/m\mathbb{Z} \to \mathbb{R}/n\mathbb{Z}$, with two functions considered equivalent if they differ by integer rotation of the domain and range circles.*

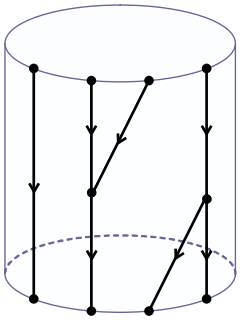

FIGURE 21. From an annular strand diagram to a cylindrical one

*Proof.* A *labeling* of a cylindrical $(m, n)$ strand diagram is a counterclockwise assignment of the numbers $1, 2, \ldots m$ to the sources, and a counterclockwise assignment of the numbers $1, 2, \ldots n$ to the sinks (see figure 22). Given

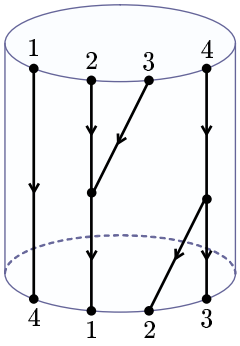


FIGURE 22. Labeling of a cylindrical strand diagram

a labeling, we can interpret the cylindrical strand diagram as a function $\mathbb{R}/m\mathbb{Z} \to \mathbb{R}/n\mathbb{Z}$, with the source labeled $k$ corresponding to the interval $[k-1, k] \subset \mathbb{R}/\mathbb{Z}$, and so forth. We claim that labeled reduced cylindrical $(m, n)$-strand diagrams are in one-to-one correspondence with Thompson-like functions $\mathbb{R}/m\mathbb{Z} \to \mathbb{R}/n\mathbb{Z}$.

The argument is similar to the proof of Theorem 1.4. Suppose we are given a Thompson-like homeomorphism $f\colon \mathbb{R}/m\mathbb{Z} \to \mathbb{R}/n\mathbb{Z}$ (see figure 23). Then we can construct a pair of binary forests representing the dyadic subdivisions of the domain and range circles (see figure 24). The forest for

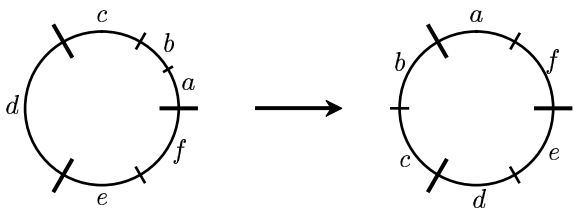


FIGURE 23. A circle map

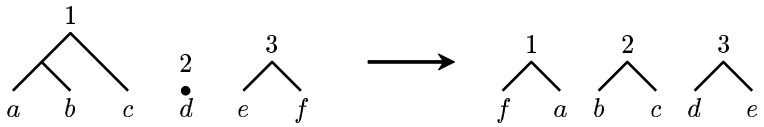


FIGURE 24. A forest diagram for the circle map

the domain has $m$ trees (corresponding to the subdivisions of the intervals $[0,1],[1,2],\dots[m-1,m]$ in $\mathbb{R}/m\mathbb{Z}$), and the forest for the range has $n$ trees. Since the function $f$ is continuous, it must preserve the cyclic order of the intervals. Therefore, we can construct a strand diagram for $f$ by attaching the leaves of the top forest to the leaves of the bottom forest via some cyclic permutation (see figure 25). This gives a labeled cylindri-

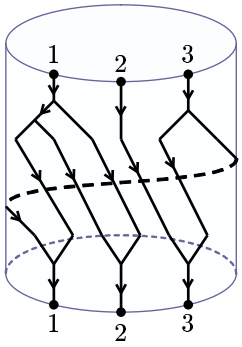


FIGURE 25. The constructed labeled cylindrical strand diagram

cal strand diagram for $f$. Conversely, given any reduced labeled cylindrical $(m,n)$-strand diagram, we can cut along every edge that goes from a split to a merge. This decomposes the cylindrical strand diagram into two forests, and therefore specifies a Thompson-like homeomorphism $f$.

Finally, note that changing the labeling of the sources of a cylindrical $(m, n)$-strand diagram has the effect of performing an integer rotation on the domain of the corresponding function. Similarly, changing the labeling of the sinks performs an integer rotation on the range. □

All that remains is the following:

**Proposition 3.8.** *Let $\mathcal{A}$ be the reduced annular strand diagram for a one-bump function $f \in F$, and let $\mathcal{C}$ be the cylindrical $(m, n)$-strand diagram obtained by removing the merge and split loops from $\mathcal{A}$. Then $\mathcal{C}$ is the cylindrical strand diagram for the Mather invariant $f^\infty \colon \mathbb{R}/m\mathbb{Z} \to \mathbb{R}/n\mathbb{Z}$.*

*Proof.* Let $f \colon [0, k] \to [0, k]$ be the one-bump function obtained by cutting a reduced annular strand diagram $\mathcal{A}$ along a cutting path $c$. Let $e_0$ and $e_1$ be the edges on the inner and outer loops crossed by $c$.

If we place a binary number along $e_0$, it will circle the split loop for a while, eventually exiting along some edge. This edge depends on the length of the initial string of zeroes in the binary expansion of the number (figure 26). In particular, a number leaves along the $i$th edge with value $.\beta$ if and

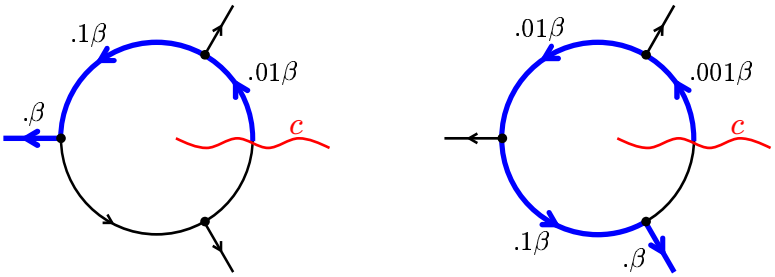


FIGURE 26. Traveling through a split loop

only if the image of the number in $\mathbb{R}/m\mathbb{Z}$ is $(i-1) + .\beta$.

After leaving the split loop, the number travels through the cylindrical strand diagram for the circle map, eventually entering the merge loop. If we stop the number when it reaches the edge $e_1$, it will have the form $.11 \cdots 10\gamma$, where $\gamma$ is the fractional part of the image of $(i-1) + .\beta$ under the circle map, and the length of the string of 1's determines the integer part. □

This completes the proof of theorem 3.6.

## ACKNOWLEDGMENTS

The authors would like to thank Ken Brown and Martin Kassabov for a very careful reading of this paper and many helpful remarks. The authors

would also like to thank Stephen Pride for providing fundamental references and Collin Bleak, Matt Brin and Mark Sapir for helpful conversations.

## References

[1] V. S. Afraimovich and T. Young. Mather invariants and smooth conjugacy on $S^2$. *J. Dynam. Control Systems*, 6(3) (2000), 341–352.

[2] G. R. Belitskiĭ. Smooth classification of one-dimensional diffeomorphisms with hyperbolic fixed points. *Sibirsk. Mat. Zh.*, 27(6)(1986), 21–24.

[3] J.M. Belk. *Thompson's Group F*. PhD thesis, Cornell University, 2004. `arXiv:math.GR/0708.3609v1`.

[4] J.M. Belk and F. Matucci. Conjugacy in Thompson's groups. *CRM preprint series*, (828), 2008. `arXiv:math.GR/0708.4250v1`.

[5] W. A. Bogley and S. J. Pride. Calculating generators of $\Pi_2$. In *Two-dimensional homotopy and combinatorial group theory*, volume 197 of *London Math. Soc. Lecture Note Ser.*, pages 157–188. Cambridge Univ. Press, Cambridge, 1993.

[6] Matthew G. Brin and Craig C. Squier. Presentations, conjugacy, roots, and centralizers in groups of piecewise linear homeomorphisms of the real line. *Comm. Algebra*, 29(10) (2001), 4557–4596.

[7] J.W. Cannon, W.J. Floyd, and W.R. Parry. Introductory notes on Richard Thompson's groups. *Enseign. Math. (2)*, 42(3-4) (1996), 15–256.

[8] N. Gill and I. Short. Conjugacy in thompson's group. *Preprint.* `arXiv:math.GR/0709.1987v2` .

[9] R. I. Grigorchuk, V. V. Nekrashevich, and V. I. Sushchanskiĭ. Automata, dynamical systems, and groups. *Tr. Mat. Inst. Steklova*, 231(Din. Sist., Avtom. i Beskon. Gruppy), 134–214, 2000.

[10] V. S. Guba and M. V. Sapir. On subgroups of the R. Thompson group $F$ and other diagram groups. *Mat. Sb.*, 190(8) (1999), 3–60.

[11] Victor Guba and Mark Sapir. Diagram groups. *Mem. Amer. Math. Soc.*, 130(620) (1997), viii+117.

[12] M. Kassabov and F. Matucci. The simultaneous conjugacy problem in groups of piecewise linear functions. *Preprint.* `arXiv:math.GR/0607167v2`.

[13] John N. Mather. Commutators of diffeomorphisms. *Comment. Math. Helv.*, 49 (1974), 512–528.

[14] F. Matucci. *Algorithms and Classification in Groups of Piecewise-Linear Homeomorphisms*. PhD thesis, Cornell University, 2008. `arXiv:math.GR/0807.2871v1`.

[15] Stephen J. Pride. Geometric methods in combinatorial semigroup theory. In *Semigroups, formal languages and groups (York, 1993)*, volume 466 of *NATO Adv. Sci. Inst. Ser. C Math. Phys. Sci.*, pages 215–232. Kluwer Acad. Publ., Dordrecht, 1995.

[16] Stephen J. Pride. Low-dimensional homotopy theory for monoids. *Internat. J. Algebra Comput.*, 5(6) (1995), 631–649.

[17] Jean-Christophe Yoccoz. Centralisateurs et conjugaison différentiable des difféomorphismes du cercle. *Astérisque*, (231) (1995), 89–242. Petits diviseurs en dimension 1.

[18] Todd R. Young. $C^k$ conjugacy of 1-D diffeomorphisms with periodic points. *Proc. Amer. Math. Soc.*, 125(7) (1997), 1987–1995.

James Belk
Mathematics Program, Bard College
Annandale-on-Hudson, NY 12504, U.S.A
*E-mail address*: belk@bard.edu

Francesco Matucci
Centre de Recerca Matemàtica,
Apartat 50, 08193 Bellaterra, Barcelona, Spain
*E-mail address*: fmatucci@crm.cat